Effect of processing routes on microstructure, phase evolution and indentation characteristics of $Fe_{56.24}Cr_4Mo_{14}C_{15}Si_{3.8}B_6$, $Fe_{43.47}Cr_{15}Mo_{14}C_{15.12}Si_{3.78}B_6Y_2$, $Fe_{40.2}Cr_{20}Mo_{10}W_2C_{15}Si_{4.2}B_6Y_2$ and $Fe_{40.2}Cr_{15}Mo_{14}Co_3C_{15}Si4._2B_6Y_2$ alloys

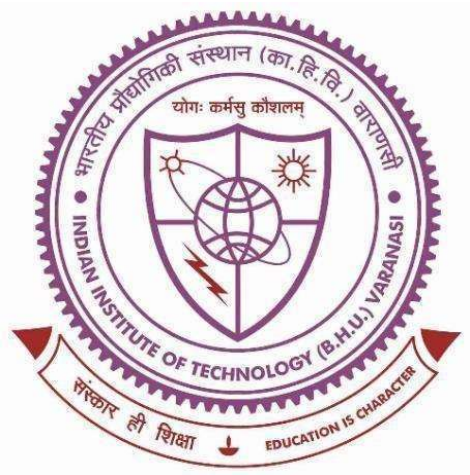

THESIS SUBMITTED FOR THE DEGREE OF

DOCTOR OF PHILOSOPHY

IN

METALLURGICAL ENGINEERING

BY

SARIKA KUMARI

DEPARTMENT OF METALLURGICAL ENGINEERING

INDIAN INSTITUTE OF TECHNOLOGY

(BANARAS HINDU UNIVERSITY)

VARANASI – 221005

INDIA

Roll No. 17141010

2024

Chapter-07: Summary and Suggestion for Future Work

7.1 Summary

The present study is based on four iron-based alloy compositions. These compositions are selected based on e/a, V_R, and R_R glass forming criteria proposed earlier. Alloys were made by copper mould casting method. They were subjected to (i) melt-spinning, and (ii) high energy ball milling. Further 100h of ball milled powder was consolidated by spark plasma sintering (SPS) technique. The X-ray diffraction studies and microstructural characterization of samples prepared through all routes are studied. Indentation behaviour was also investigated. The major findings from various chapters of this doctoral thesis are given below:

7.1.1 Synthesis and characterization of as-cast alloys

The vacuum arc melting followed by Cu-mould casting technique was initially used to prepare four different Fe-based alloys in the form of disc. These alloys are having uniform microstructure throughout the sample except alloy-A ($Fe_{56.24}Cr_4Mo_{14}C_{15}Si_{3.8}B_6$). Alloy-A have non-uniform microstructure of dendrites and pearlite. These alloys are fully crystalline in nature, confirmed by X-ray diffraction analysis. The phases evolved in these alloys are α-Fe (cI2), $Fe_{11}Mo_6C_5$ (mC44), Cr_7C_3 (oP40), Fe_5C_2 (mC28), Fe_3C (oP116) and Fe_3W_3C (cF112). Some of the phases are common in them. Some of these phases are also observed in various amorphous steels in literature too, after annealing process. The minimum and maximum melting temperature of alloy-A and alloy-D are 1035°C and 1145°C respectively. Such a change is owing to alloying addition.

The Vickers micro-indentation experiment was carried out for indentation behaviour analysis. The hardness versus load relation tells about indentation size effect. In all the as-cast alloys hardness increases with load and become constant after the failure (i.e. RISE observed). Among all the alloys, alloy-D ($Fe_{40.2}Cr_{15}Mo_{14}Co_3C_{15}Si4.2B_6Y_2$) has maximum hardness (VHN= ~1327) and Yield strength (σ_o=9.26 GPa). It may be due to finer microstructure observed in this alloy. The Palmqvist type of cracks is observed in alloy-B and alloy-D at 1000g and 500g load respectively, while cracks are absence in alloy-A and alloy-C till these loads. The absence of cracks displays relatively better resistance to crack propagation in them. The average fracture toughness in alloy-B and alloy-D are found to be 4.22 MPa.$m^{1/2}$ and 3.73 MPa.$m^{1/2}$respectively.

It was observed from that, the elastic recovery ($R=h_f/h_{max}$) for as-cast alloys are in the range of 0.66 to 0.77, while percentage of elastic recovery (%R) ranges between ~29% to 33%. The ratio

of hardness to elastic modulus (H/E) is obtained maximum for alloy-D (~ 0.049). The maximum value of H/E, indicate that the elastic recovery is more in the alloy-D. The hardness to density ratio (H/ρ) and specific stiffness (E/ρ) are found maximum for alloy-D 1.78 and 36 respectively. It has been observed that the H/ρ ratio of present alloy was found ~ 4 times higher than maraging steel and it is comparable to amorphous steel as bulk metallic glass. The E/ρ is higher than that of maraging steel (~19) and comparable to amorphous steel (~32).

7.1.2 Glass/glass-nanocomposites formation in Fe-based alloys

Glass formation takes place only in MS-A and MS-D, while MS-B and MS-C have displayed glass-nanocomposites phase formation after melt-spinning. The nanocrystallites of α-Fe (cI2) and $Fe_{11}Mo_6C_5$ (mC44) are embedded in the glassy matrix of melt-spun ribbons. Melt-spun ribbon MS-A and MS-C exhibits the glass transition temperature behaviour. The glass transition temperatures of these ribbons are 600 ^oC and 609 ^oC respectively. The GFA parameters ΔT_x and T_{rg} of these samples suggests high thermal stability of the present alloys.

As-synthesized melt-spun ribbons and annealed ribbons show indentation size effect (ISE). A more significant ISE has been observed in the annealed ribbon as compared to as-synthesized ribbons. It was observed that MS-A exhibits maximum microhardness value (~ 11.5 GPa) at 100g load and after annealing AMS-C exhibits maximum microhardness (~14GPa) at 75g of indentation load. Shear bands formation was observed in the melt-spun ribbons which are the characteristics of amorphous phase. The H/E ratio of MS-D (~0.21) and AMS-B (~0.28) displays maximum values.

7.1.3 Phase evolution and Indentation of Ball milled powder/ Pellets

Alloys prepared by Cu-mould casting were also used for high energy ball milling. Small granules of these alloys milled up to 120h but it was observed that no further change in phase evolution takes place after 100h of milling. The morphology of ball-milled powders of sample BMP-A and BMP-B changes with milling time and it was seen that at the end of milling (i.e. 100h) spherical morphology achieved. Although in case of powder of BMP-C and BMP-D the faceted morphology obtained. This may be due to tungsten and cobalt addition in sample B composition. The α-Fe and $Fe_{11}Mo_6C_5$ are retained in the ball milled powders at the end of milling. Further, 100h of ball-milled powders consolidated through SPS technique gave some new crystalline phases $Fe_{23}C_6$ and $FeMo_2B_2$ in addition to the above.

The indentation result of sintered alloys shows that among all the sintered alloys SPSed-C has highest microhardness (~11 GPa) and Young's modulus (~206GPa) values. The 0.2% offset yield

strength was calculated and found to be maximum for SPSed-D (~8GPa) at 100g load. The indentation depth was found maximum for SPSed-A alloy (~3.22μm). Therefore, the minimum hardness is obtained (~3GPa). One of the main reasons for getting poor hardness in SPSed-A alloy is its poor densification. The Palmqvist type of crack is observed in SPSed-C and SPSed-D alloys at 1000g load. The average indentation fracture toughness in these sintered alloys was obtained ~3.6 MPa.$m^{1/2}$ and 3.22 MPa.$m^{1/2}$ respectively. The absence of crack around the indented area of SPSed-B, indicates more resistance to crack propagation as compared to others.

7.2 Scope and suggestion for future work

Scope and suggestions for future work should include the following aspects:

- All the compositions have shown promise in view of the H/ρ ratio. Therefore, it is suggested that they may be considered for BMGs formation by Suction casting or other methods. Such an exercise will enable the researcher to access the glass forming ability in terms of thickness of BMGs.
- A controlled atmosphere melt-spinner may be used for better quality of ribbons.